*Carbohydrate Research*, 224 (1992) 1–17
Elsevier Science Publishers B.V., Amsterdam



# Roles of potassium ions, acetyl and L-glyceryl groups in native gellan double helix: an X-ray study

Rengaswami Chandrasekaran*, Akella Radha, and Vadakkanthara G. Thailambal
*Whistler Center for Carbohydrate Research, Smith Hall, Purdue University, West Lafayette, IN 47907 (U.S.A.)*

(Received April 1st, 1991; accepted for publication June 20th, 1991)

ABSTRACT

Native gellan, the natural form of the polysaccharide excreted by the bacterium *Pseudomonas elodea*, has a tetrasaccharide repeating unit that contains L-glyceral and acetate ester groups, and forms only weak and elastic gels. Based on X-ray diffraction data from well oriented and polycrystalline fibers of its potassium salt, the crystal structure of native gellan, including ions and water, has been determined and refined to a final *R*-value of 0.17. The molecule forms a half-staggered, parallel, double helix of pitch 5.68 nm which is stabilized by hydrogen bonds involving the hydroxymethyl groups in one chain and both carboxylate and glyceryl groups in the other. Two molecules are packed in an antiparallel fashion in a trigonal unit cell of side $a = 1.65$ nm. Although the gross molecular morphology and packing arrangements are isomorphous with those observed in the crystal structure of potassium gellan, which is devoid of any substitutions, native gellan exhibits exceptional changes in its ion binding characteristics with respect to gellan. In particular, the L-glyceryl groups do not allow the gellan-like coordinated interactions of the ions and the carboxylate groups, within and between double helices, which are necessary for strong gelation. These results at the molecular level explain, for the first time, the differences in the behavior of the polymer with and without substitutions.

## INTRODUCTION

The gellan family of microbial polysaccharides consisting of gellan, native gellan, welan, S-657, rhamsan, and others are of considerable importance because of their good gelling properties or high viscosity in aqueous solutions[1,2]. The commercial gellan gum is a linear acidic polysaccharide and carries no substitution. Its repeating unit is a tetrasaccharide[3], ABCD, given by

→3)-β-D-Glc*p*-(1→4)-β-D-Glc*p*A-(1→4)-β-D-Glc*p*-(1→4)-α-L-Rha*p*-(1→.

Gellan forms strong and brittle gels in the presence of monovalent or divalent cations[4]. The other members in the family have the same tetrasaccharide as the backbone repeating unit which in addition has simple substitutions of L-glyceral and acetyl groups in native gellan[5] or mono- and di-saccharides in welan, S-657 and rhamsan[1]. Solution studies[1,6,7] to date indicate that there is considerable weakening, or complete depletion, of gelation behavior of the polymer depending on the extent of substitution.

* Author for correspondence.

0008-6215/92/$ 05.00 

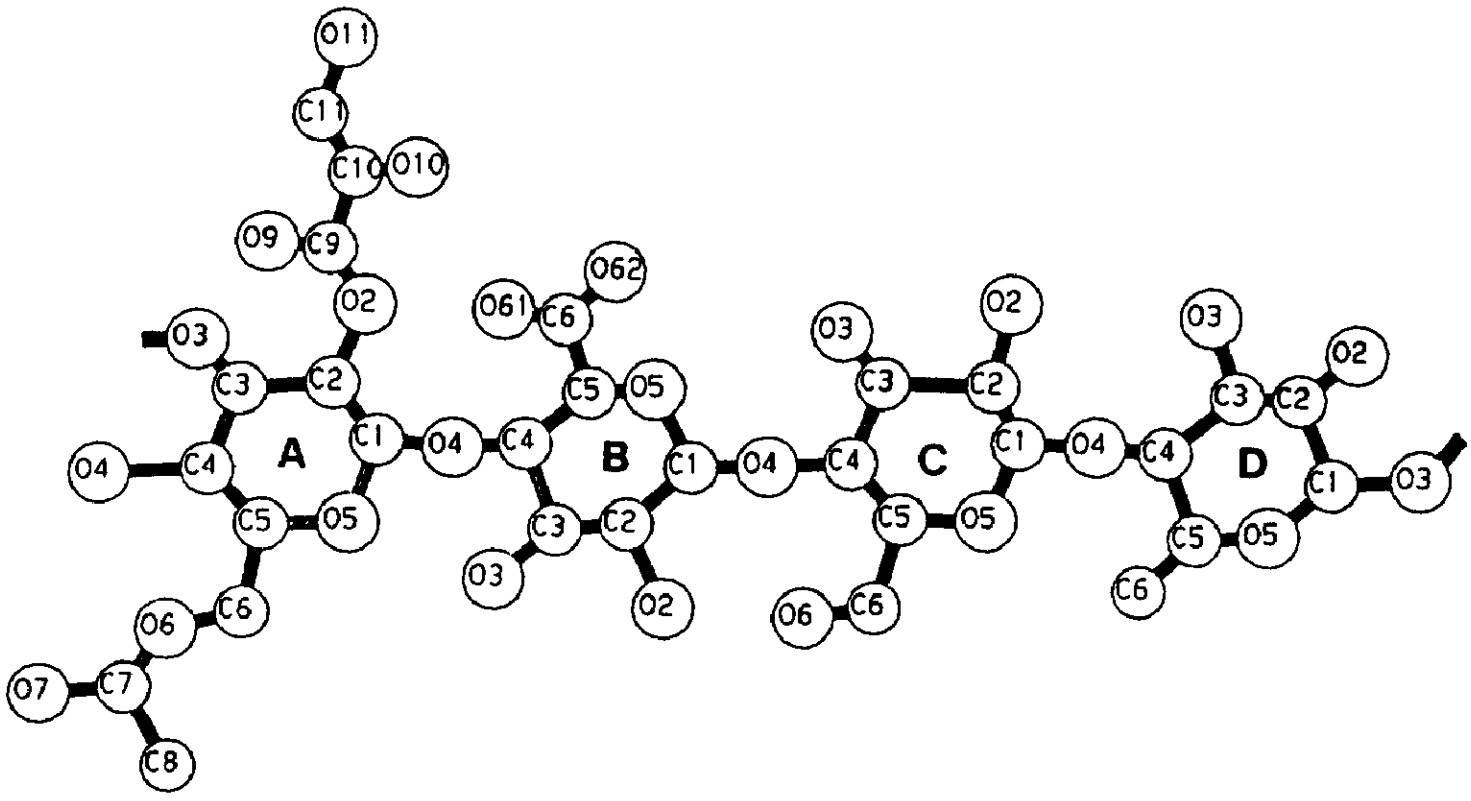


Fig. 1. Schematic representation and atom labeling of the tetrasaccharide repeating unit of native gellan. The glucose unit A has L-glyceryl substitution at O-2 and acetyl at O-6.

One of our ongoing research projects is to investigate the structural roles of the side chains on the observed rheological properties. Earlier, we have demonstrated that gellan itself forms a half-staggered, parallel, double helix with 3-fold left-handed polysaccharide chains[8]. In the case of native gellan, as its repeating unit (Fig. 1) shows, glucose A has one or two substitutions[5], the L-glyceryl group at O-2, and acetyl group of half occupancy at O-6. We speculated from computer-modeling studies[9] that the polymer would adopt a double helix similar to that of gellan in which the glyceryl groups would not permit the gellan-type of intermolecular aggregation[8] that is required for strong gelation to occur. Now we have successfully carried out a detailed crystal-structure analysis of the potassium salt in fibers. The results are in good agreement with the predictions[9] and can explain the formation of weak and rubbery gels of native gellan in aqueous solutions. In addition, its packing arrangement has enabled us to propose a putative model for its calcium salt, for which we do not yet have any good X-ray diffraction patterns. This model involves the direct cross-linking of native gellan double helices *via* calcium ions similar to that of calcium gellan[9].

## EXPERIMENTAL

*Fiber preparation.* — Samples of native gellan were provided by Dr. Ralph Moorhouse (Kelco, Division of Merck, San Diego, CA). An aqueous solution (0.3 mg/mL) was prepared at 70° with constant stirring and dialysed against 20mM KF at room temperature. Excess salt, if any, was removed by further dialysis against distilled water.

A small amount of the polysaccharide solution was placed in the gap between the two glass rods in a conventional fiber puller and 1 $\mu$L of 10mM KOAc adjusted to pH 7.3 was added to it. This was helpful to keep the drop from breaking apart. After mixing, the drop was allowed to dry slowly, and stretched to achieve orientation along the fiber axis. The density of the fiber was measured by the flotation method using a mixture of bromobenzene and bromoform.

*X-Ray intensity data.* — Diffraction patterns were recorded on flat photographic films in pin-hole cameras using Ni-filtered Cu$K_\alpha$ radiation ($\lambda$ = 0.15418 nm) from a sealed-tube Philips generator operated at 40 kV and 25 mA. Typical sample-to-film distance was 35 mm. A steady stream of helium gas, after bubbling through appropriate saturated salt solution, was used to flush the specimen chamber in order to maintain the fiber at the desired relative humidity. The unit-cell dimensions were measured using patterns obtained from polycrystalline and oriented fibers dusted with calcite powder (of characteristic spacing 0.3035 nm) for internal calibration.

The diffraction pattern was digitized by using an Optronics P-1000 rotating drum microdensitometer with a 50-$\mu$m raster step. The digitized pattern was processed using a VAX 11/750 and a Lexidata raster graphics system. Based on points selected between layer lines, and away from the spots, the background in the film was estimated[10] and subtracted from the entire pattern. The radial and angular profiles of a few sharp Bragg spots in the background corrected pattern were used to determine the crystallite size and disorientations in the specimen for defining the reflection boundaries. The Bragg intensities were calculated by integrating the optical densities inside each spot bounda-

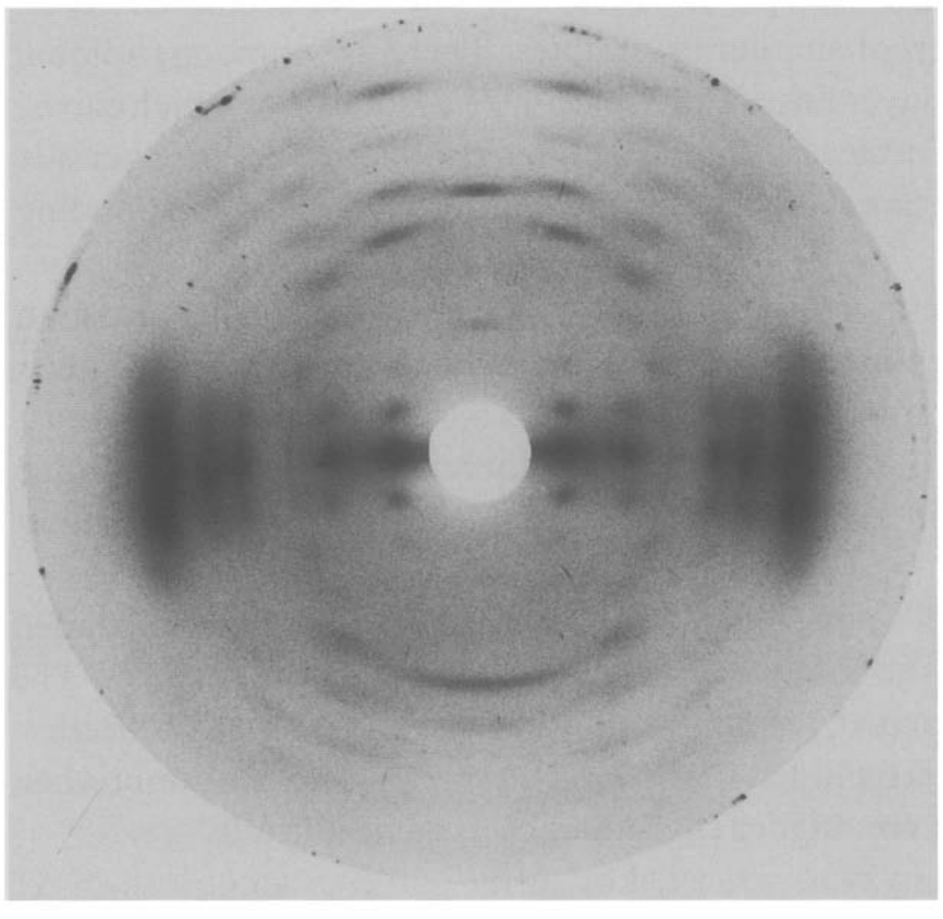

Fig. 2. X-Ray diffraction pattern from a well oriented and polycrystalline fiber of the potassium salt of native gellan maintained at 75% relative humidity.

ry[11]. Lorentz and polarization corrections were applied before computing the observed structure amplitudes.

*Model building and structure analysis.* — Molecular models, consistent with the helix symmetry and *c*-repeat as observed in the X-ray diffraction pattern (Fig. 2), were constructed using the linked-atom least-squares procedure[12]. In the initial stages of structure analysis, the sugar rings in the repeating unit were treated as rigid bodies and only the conformation angles around the glycosidic bonds, and of the side groups were allowed to vary. In the final stages, the endocyclic conformation and bond angles in the rings were also refined.

Structure factors calculated with the atomic scattering factors given in the International Tables of Crystallography[13] were used to compute difference Fourier maps having $(2F_o - F_c)$ as coefficients, at various stages of the refinement process. The maps were not only helpful to locate cations and water molecules in the unit cell, but also enabled us to fix the side group conformations unequivocally. In all remaining calculations, water-smeared scattering factors[14] were employed to account for the solvent in the unit cell and the *R*-values are given on this basis. Hamilton's significance test[15] was used to arbitrate between alternative hypotheses on guest molecules identified in difference Fourier maps and on their occupancies. The least-squares refinements were continued until convergence so that the final model was sterically satisfactory and provided good fit with the observed X-ray data.

*Diffraction pattern and unit-cell contents.* — The diffraction pattern of native gellan shown in Fig. 2 corresponds to 75% relative humidity. The sharpness of the spots fades as the relative humidity is changed. The intensity distribution and layer line spacings are of the same kind as those from potassium gellan, but the spot size, however, corresponds to specimens made up of smaller crystallites. There are three meridional reflections on the 3rd, 6th, and 9th layer lines, and 31 non-meridional spots which can be indexed with a trigonal unit cell of dimensions (and estimated standard deviations) $a = b = 1.647(5)$ nm and $c = 2.842(7)$ nm, which are slightly larger than the corresponding values for potassium gellan[8], $a = b = 1.575$ nm and $c = 2.815$ nm. The similarities confirm that the two crystal structures are isomorphous. Therefore, as in potassium gellan, the native gellan molecule must also be a half-staggered, parallel, double helix with 3-fold left-handed polysaccharide chains of pitch $(2c)$ 5.68 nm. The unit cell must contain two double helices. To account for the measured fiber density of 1.57 g/mL, one may expect to find a potassium ion and about 15 water molecules for every repeating unit.

A set of 17 "below threshold" spots, which are too weak to be seen, was appended to the list of 31 observed spots in the X-ray data in conducting structure analysis. The lowest measured intensity was assigned, as the threshold value, to each weak reflection in this group. Such a reflection was included in the least-squares refinement only when its calculated structure amplitude was higher than the observed amplitude.

## DEVELOPMENT OF THE CRYSTAL STRUCTURE

The conformation of the native gellan double helix used in the initial crystal-packing arrangement, of space group $P3_1$, was the same as reported in our previous computer modeling study[9]. Two double helices, I and II, were positioned at (2/3, 1/3) and (1/3, 2/3) in antiparallel fashion. A survey of the intermolecular contacts between the double helices, conducted in the ($\mu_1$, $\mu_2$, $w_2$) space, where the variables are the packing parameters ($\mu_1$ for molecule I, and $\mu_2$ and $w_2$ for II), showed that the best situation was essentially similar to that in the potassium gellan crystal structure[8]. The *R*-value for this starting model was 0.33. The first ($2\rho_o - \rho_c$) map computed for the polyanion crystal-structure confirmed that the acetyl group was in the correct orientation, but the glyceryl group, including and beyond C-10A (Fig. 1), had to be oriented differently. Incorporation of this change reduced the *R*-value to 0.29. In the course of three difference maps, five water molecules, each hydrogen bonding with at least two polyanion oxygen atoms, could be located unambiguously in a third of the unit cell that comprises the crystallographic asymmetric unit. The fourth difference map, computed with the augmented crystal structure, showed a peak in the vicinity of the carboxylate group of molecule I and similarly one for molecule II. Each could serve as a potassium ion. The three oxygen atoms O-62B, O-5B, and O-3C, all in one strand of the double helix, were at coordinating distances from this putative cation site.

The height of either peak was somewhat smaller than those of the water molecules previously identified. If the peak were indeed a potassium ion, its occupancy could be less than one; or it could just be another water molecule. These possibilities were examined as follows: the guest atom was included in the crystal structure as a full potassium, half a potassium, or a water molecule. The respective *R*-values, were 0.215, 0.177, and 0.180. Comparison of the *R*-values suggested that the assignment of the peak as half a potassium ion is superior to a full potassium at 99.5% confidence level[15]. On the other hand, a similar assertion *vis-a-vis* a water molecule could be made only at a lower (75%) confidence level. The above tests were based on 42 spots in the X-ray data-set that were used in the least-squares refinement as observations; the type of the scattering factor of the guest atom was the only variable. Although discrimination between half a potassium and a water molecule was only marginal, we assigned this peak to half a potassium. This choice is compatible with the primary structure and the implications are discussed later. Additional cations or water molecules could not be located from subsequent maps. By relaxing the sugar rings in the final rounds of crystal structure refinement, the *R*-value slightly decreased to 0.17. The atomic coordinates of the final model of native gellan double helix, cations, and water molecules are given in Table I. The observed and calculated structure factors are listed in Table II.

## STRUCTURAL FEATURES

*Polyanion conformation.* — The major conformation angles in a repeating unit of the native gellan double helix are listed in Table III. Their estimated standard devia-

TABLE I

Cartesian and cylindrical polar coordinates for a tetrasaccharide repeating-unit in the native gellan double helix, cations and water molecules[a]

| *Group* | *Atom* | *X (nm)* | *Y (nm)* | *Z (nm)* | *r (nm)* | *φ(°)* |
|---|---|---|---|---|---|---|
| Residue A | C-1 | −0.1439 | −0.3101 | 1.5217 | 0.3419 | −114.90 |
| | C-2 | −0.1290 | −0.2519 | 1.6617 | 0.2830 | −117.12 |
| | C-3 | −0.1794 | −0.3531 | 1.7634 | 0.3960 | −116.94 |
| | C-4 | −0.3230 | −0.3922 | 1.7312 | 0.5081 | −129.48 |
| | C-5 | −0.3330 | −0.4396 | 1.5866 | 0.5514 | −127.14 |
| | C-6 | −0.4756 | −0.4673 | 1.5439 | 0.6667 | −135.50 |
| | C-7 | −0.6521 | −0.6179 | 1.5903 | 0.8983 | −136.54 |
| | C-8 | −0.7118 | −0.6271 | 1.4519 | 0.9486 | −138.62 |
| | C-9 | 0.0954 | −0.3126 | 1.7153 | 0.3269 | −73.03 |
| | C-10 | 0.2272 | −0.2582 | 1.7685 | 0.3439 | −48.65 |
| | C-11 | 0.2136 | −0.2148 | 1.9130 | 0.3029 | −45.16 |
| | O-2 | 0.0074 | −0.2185 | 1.6844 | 0.2186 | −88.06 |
| | O-3 | −0.1715 | −0.2971 | 1.8947 | 0.3430 | −120.00 |
| | O-4 | −0.3663 | −0.4976 | 1.8169 | 0.6179 | −126.36 |
| | O-5 | −0.2817 | −0.3392 | 1.4976 | 0.4409 | −129.71 |
| | O-6 | −0.5215 | −0.5964 | 1.5839 | 0.7922 | −131.17 |
| | O-7 | −0.7127 | −0.6284 | 1.6956 | 0.9502 | −138.60 |
| | O-9 | 0.0727 | −0.4318 | 1.7021 | 0.4379 | −80.44 |
| | O-10 | 0.2704 | −0.1458 | 1.6933 | 0.3072 | −28.34 |
| | O-11 | 0.2559 | −0.3190 | 2.0011 | 0.4089 | −51.27 |
| | H-1 | −0.0850 | −0.4026 | 1.5137 | 0.4115 | −101.91 |
| | H-2 | −0.1869 | −0.1586 | 1.6689 | 0.2451 | −139.68 |
| | H-3 | −0.1155 | −0.4424 | 1.7578 | 0.4572 | −104.63 |
| | H-4 | −0.3889 | −0.3054 | 1.7462 | 0.4945 | −141.86 |
| | H-5 | −0.2751 | −0.5323 | 1.5743 | 0.5992 | −117.33 |
| | H-61 | −0.5422 | −0.3910 | 1.5867 | 0.6684 | −144.20 |
| | H-62 | −0.4833 | −0.4591 | 1.4345 | 0.6666 | −136.47 |
| | H-81 | −0.6756 | −0.7183 | 1.4022 | 0.9861 | −133.24 |
| | H-82 | −0.8215 | −0.6306 | 1.4594 | 1.0356 | −142.49 |
| | H-83 | −0.6820 | −0.5390 | 1.3931 | 0.8692 | −141.68 |
| | H-10 | 0.3044 | −0.3363 | 1.7623 | 0.4536 | −47.86 |
| | H-111 | 0.1084 | −0.1906 | 1.9343 | 0.2193 | −60.38 |
| | H-112 | 0.2759 | −0.1258 | 1.9306 | 0.3032 | −24.52 |
| Residue B | C-1 | 0.0368 | −0.2159 | 1.0398 | 0.2190 | −80.33 |
| | C-2 | −0.0592 | −0.3287 | 1.0753 | 0.3340 | −100.20 |
| | C-3 | −0.1343 | −0.2955 | 1.2034 | 0.3246 | −114.43 |
| | C-4 | −0.0358 | −0.2612 | 1.3144 | 0.2636 | −97.81 |
| | C-5 | 0.0605 | −0.1527 | 1.2675 | 0.1642 | −68.37 |
| | C-6 | 0.1679 | −0.1216 | 1.3697 | 0.2073 | −35.92 |
| | O-2 | −0.1495 | −0.3495 | 0.9673 | 0.3801 | −113.15 |
| | O-3 | −0.2141 | −0.4074 | 1.2425 | 0.4602 | −117.73 |
| | O-4 | −0.1053 | −0.2137 | 1.4295 | 0.2382 | −116.23 |
| | O-5 | 0.1278 | −0.1954 | 1.1480 | 0.2335 | −56.81 |
| | O-61 | 0.1970 | −0.2096 | 1.4536 | 0.2876 | −46.76 |
| | O-62 | 0.2262 | −0.0111 | 1.3706 | 0.2265 | −2.80 |
| | H-1 | −0.0202 | −0.1235 | 1.0218 | 0.1252 | −99.28 |
| | H-2 | −0.0026 | −0.4221 | 1.0887 | 0.4221 | −90.36 |
| | H-3 | −0.2011 | −0.2100 | 1.1856 | 0.2908 | −133.76 |
| | H-4 | 0.0209 | −0.3517 | 1.3405 | 0.3523 | −86.60 |
| | H-5 | 0.0046 | −0.0601 | 1.2473 | 0.0603 | −85.65 |

| | | | | | | |
|---|---|---|---|---|---|---|
| Residue C | C-1 | 0.1868 | −0.1221 | 0.5465 | 0.2231 | −33.18 |
| | C-2 | 0.1568 | −0.0120 | 0.6473 | 0.1573 | −4.37 |
| | C-3 | 0.1700 | −0.0671 | 0.7885 | 0.1828 | −21.55 |
| | C-4 | 0.0823 | −0.1904 | 0.8060 | 0.2075 | −66.62 |
| | C-5 | 0.1075 | −0.2905 | 0.6937 | 0.3098 | −69.69 |
| | C-6 | 0.0107 | −0.4069 | 0.6965 | 0.4071 | −88.49 |
| | O-2 | 0.2459 | 0.0969 | 0.6259 | 0.2643 | 21.50 |
| | O-3 | 0.1314 | 0.0330 | 0.8828 | 0.1354 | 14.08 |
| | O-4 | 0.1117 | −0.2551 | 0.9296 | 0.2785 | −66.35 |
| | O-5 | 0.0926 | −0.2280 | 0.5653 | 0.2461 | −67.89 |
| | O-6 | −0.1241 | −0.3642 | 0.6772 | 0.3848 | −108.81 |
| | H-1 | 0.2887 | −0.1604 | 0.5620 | 0.3303 | −29.06 |
| | H-2 | 0.0548 | 0.0259 | 0.6311 | 0.0606 | 25.27 |
| | H-3 | 0.2749 | −0.0939 | 0.8077 | 0.2905 | −18.86 |
| | H-4 | −0.0231 | −0.1591 | 0.8052 | 0.1608 | −98.27 |
| | H-5 | 0.2095 | −0.3308 | 0.7027 | 0.3915 | −57.66 |
| | H-61 | 0.0379 | −0.4791 | 0.6180 | 0.4806 | −85.47 |
| | H-62 | 0.0192 | −0.4594 | 0.7928 | 0.4598 | −87.61 |
| Residue D | C-1 | 0.4334 | 0.0141 | 0.1064 | 0.4337 | 1.87 |
| | C-2 | 0.3870 | 0.1289 | 0.1953 | 0.4079 | 18.42 |
| | C-3 | 0.2583 | 0.0908 | 0.2670 | 0.2738 | 19.36 |
| | C-4 | 0.2852 | −0.0358 | 0.3471 | 0.2874 | −7.16 |
| | C-5 | 0.3280 | −0.1471 | 0.2503 | 0.3594 | −24.16 |
| | C-6 | 0.3615 | −0.2777 | 0.3198 | 0.4558 | −37.54 |
| | O-2 | 0.4913 | 0.1564 | 0.2879 | 0.5156 | 17.66 |
| | O-3 | 0.2207 | 0.2015 | 0.3466 | 0.2989 | 42.39 |
| | O-4 | 0.1673 | −0.0719 | 0.4184 | 0.1820 | −23.25 |
| | O-5 | 0.4470 | −0.1060 | 0.1807 | 0.4594 | −13.34 |
| | H-1 | 0.5299 | 0.0396 | 0.0601 | 0.5314 | 4.28 |
| | H-2 | 0.3700 | 0.2184 | 0.1337 | 0.4297 | 30.55 |
| | H-3 | 0.1792 | 0.0721 | 0.1929 | 0.1932 | 21.93 |
| | H-4 | 0.3666 | −0.0163 | 0.4183 | 0.3670 | −2.54 |
| | H-5 | 0.2475 | −0.1653 | 0.1775 | 0.2977 | −33.74 |
| | H-61 | 0.2713 | −0.3406 | 0.3252 | 0.4354 | −51.45 |
| | H-62 | 0.4396 | −0.3305 | 0.2630 | 0.5499 | −36.94 |
| | H-63 | 0.3978 | −0.2569 | 0.4215 | 0.4736 | −32.85 |
| Ion & water | K-1 | −0.0316 | 0.2065 | 1.1201 | 0.2080 | 98.69 |
| | K-2 | −0.2242 | 0.7948 | 1.1223 | 0.8258 | 105.75 |
| | W-1 | −0.8233 | 0.3143 | −0.4991 | 0.8813 | 159.10 |
| | W-2 | 0.4647 | 0.2084 | −0.5906 | 0.5093 | 24.16 |
| | W-3 | 0.3296 | −0.5808 | −0.5985 | 0.6679 | −60.42 |
| | W-4 | −0.4947 | −0.4062 | −0.4923 | 0.6401 | −140.61 |
| | W-5 | 0.3153 | 0.1611 | −0.3781 | 0.3541 | 27.07 |

[a] The $a^*$-axis in the unit-cell defines $\varphi = 0°$ and $r = 0$ is the helix axis. In the crystal structure, after applying the final packing parameters, double helix I has cylindrical polar coordinates $(r, \varphi + 76.8°, Z)$ and its helix axis passes through (2/3, 1/3); and similarly, double helix II has coordinates $(r, -\varphi + 5.8°, -Z - 0.594\,\text{nm})$ and its helix axis passes through (1/3, 2/3). Successive repeating units, which alternate between the two chains, in the double helix can be obtained from the new values of $(r, \varphi, Z)$, by adding multiples of 120° to $\varphi$, and the same multiple of 0.947 nm to $Z$. Coordinates of all the ions and water molecules in a third of the unit cell are given, for convenience, with respect to the double helix I already positioned at (2/3, 1/3). Their symmetry mates can be generated by adding multiples of 120° to $\varphi$ and the same multiple 0.947 nm to $Z$, and brought into the unit cell by $a$ and $b$ translations as necessary.

TABLE II

Structure amplitudes for the potassium salt of native gellan (a) scaled observed, and (b) calculated

**a**

| h | k | l = 0 | 1 | 2 | 3 | 4 | 5 | 6 | 7 | 8 | 9 |
|---|---|---|---|---|---|---|---|---|---|---|---|
| 0 | 0 | M | N | N | M | N | N | M | N | N | M |
| 1 | 0 | 226 | 161 | 89 | (60) | (63) | 136 | 119 | 65 | 175 | (87) |
| 1 | 1 | 192 | 152 | (71) | 115 | 143 | | | | | |
| 2 | 0 | 145 | 148 | 157 | (82) | (85) | 167 | 144 | 132 | 142 | |
| 2 | 1 | 410 | 321 | 184 | 110 | 139 | | | | | |
| 3 | 0 | 566 | 448 | (116) | (118) | (121) | 243 | 310 | (188) | (134) | |
| 2<br>3 | 2<br>1 | 567 | 630 | 397 | 405 | | (193) | (202) | | | |
| 4 | 0 | (161) | (160) | (160) | (163) | | | | | | |

**b**

| h | k | l = 0 | 1 | 2 | 3 | 4 | 5 | 6 | 7 | 8 | 9 |
|---|---|---|---|---|---|---|---|---|---|---|---|
| 0 | 0 | (1009) | 0 | 0 | (106) | 0 | 0 | (58) | 0 | 0 | (32) |
| 1 | 0 | 396 | 219 | 83 | (100) | (96) | 116 | 99 | 121 | 175 | (95) |
| 1 | 1 | 212 | 209 | (50) | 135 | 65 | | | | | |
| 2 | 0 | 146 | 97 | 103 | (101) | (109) | 170 | 170 | 162 | 163 | |
| 2 | 1 | 406 | 330 | 188 | 160 | 182 | | | | | |
| 3 | 0 | 526 | 356 | (163) | (143) | (16) | 228 | 304 | (202) | (143) | |
| 2<br>3 | 2<br>1 | 536 | 521 | 415 | 299 | | (245) | (203) | | | |
| 4 | 0 | (172) | (116) | (133) | (162) | | | | | | |

[a] M and N are meridional and systematically absent spots respectively. The structure amplitudes for the below-threshold reflections are given in parentheses. An isotropic attenuation factor $\exp(-0.06\sin^2\theta/\lambda^2)$ was applied to all the calculated amplitudes.

tions, given in parentheses, are generally less than 4°. Consequently, those for the non-bonded distances such as hydrogen bonds are typically 0.01 nm. Comparison with the potassium gellan double helix[8] (Table III) suggests that most of the main-chain conformation angles in the two cases are in the same domains; also, the introduction of glyceryl and acetyl groups has not created any major conformational changes. The largest change is ~24° for $\psi_1$ and this is necessary to accommodate the glyceryl group. The second largest difference of 20° for $\varphi_3$ appears to be caused by the new position of potassium. The difference of 14° for $\chi_2$, 24° in native gellan *vs.* 10° in potassium gellan, is further necessary in order that the glyceryl group can be positioned near the carboxylate group without steric hindrance. A side view of the double helix is shown in Fig. 3. As expected[9], the acetyl groups are on the periphery with the terminal hydrogen atom H-82 farthest from the helix axis (see Table I). On the other hand, atoms of the glyceryl moiety are in the interior, making intimate contacts within and between polymer chains.

TABLE III

Major conformation angles in the potassium native gellan double helix (this study) compared with those in potassium gellan[8]

| *Conformation angle* | *Native gellan* | *Gellan* | *Remarks* |
|---|---|---|---|
| $\varphi_1$(O-5D–C-1D–O-3A–C-3A) | −119°(2) | −124° | α-(1→3) |
| $\psi_1$(C-1D–O-3A–C-3A–C-4A) | 64°(2) | 88° | α-(1→3) |
| $\chi_1$(C-4A–C-5A–C-6A–O-6A) | −82°(4) | −79° | hydroxymethyl |
| $\theta_2$(C-5A–C-6A–O-6A–C-7A) | 159°(4) | — | acetyl |
| $\theta_3$(C-6A–O-6A–C-7A–C-8A) | 73°(4) | — | acetyl |
| $\theta_4$(O-6A–C-7A–C-8A–H-81A) | 68°(4) | — | acetyl |
| $\theta_5$(C-1A–C-2A–O-2A–C-9A) | −79°(2) | — | glyceryl |
| $\theta_6$(C-2A–O-2A–C-9A–C-10A) | −166°(2) | — | glyceryl |
| $\theta_7$(O-2A–C-9A–C-10A–C-11A) | 78°(3) | — | glyceryl |
| $\theta_8$(C-9A–C-10A–C-11A–O-11A) | 96°(4) | — | glyceryl |
| $\varphi_2$(O-5A–C-1A–O-4B–C-4B) | −99°(2) | −101° | β-(1→4) |
| $\alpha_2$(C-1A–O-4B–C-4B–C-5B) | −150°(2) | −136° | β(1→4) |
| $\psi_2$(C-4B–C-5B–C-6B–O-61B) | 24°(4) | 10° | carboxylate |
| $\varphi_3$(O-5B–C-1B–O-4C–C-4C) | −134°(3) | −154° | β-(1→4) |
| $\psi_3$(C-1B–O-4C–C-4C–C-5C) | −148°(2) | −144° | β-(1→4) |
| $\chi_3$(C-4C–C-5C–C-6C–O-6C) | 62°(3) | 58° | hydroxymethyl |
| $\varphi_4$(O-5C–C-1C–O-4D–C-4D) | −141°(3) | −150° | β-(1→4) |
| $\psi_4$(C-1C–O-4D–C-4D–C-5D) | 98°(2) | 86° | β-(1→4) |
| $\chi_4$(C-4D–C-5D–C-6D–H-61D) | 91°(4) | 77° | methyl |

*Intrachain hydrogen bonds.* — The acetyl groups have no role in hydrogen-bond formation, whereas the glyceryl groups do. The first two hydrogen bonds listed in Table IV are the same as in potassium gellan. The third and fourth, O-4A···O-5D and O-3D···O-2C are, however, new and they arise because of small coordinated variations in the backbone conformations relative to potassium gellan. The loss of O-2A···O-61B, due to glyceryl substitution at O-2A, is compensated by the fifth hydrogen bond O-10A···O-61B. Another important contribution from the glyceryl group is the sixth O-11A···O-3D hydrogen bond. These interactions provide stiffness to the polysaccharide chains.

*Interchain hydrogen bonds.* — Like gellan, the native gellan double helix also exhibits hydroxymethyl-to-carboxylate O-6C···O-62B (0.308 nm) interchain hydrogen bonds, even though its carboxylate groups are further rotated about the C-5B–C-6B bonds. This highlights the importance of this interaction for the stability of the double helix. Within the double helix, atom O-10A participates, as an acceptor, in two bifurcated hydrogen bonds, O-6C···O-10A (0.255 nm) and O-2B···O-10A (0.311 nm). Together, the three interchain hydrogen bonds provide stability to the native gellan double helix. It may be seen from Fig. 3 that the carboxylate group is surrounded by a number of oxygen atoms. This shielding might permit partial protonation of the carboxylate group.

*Potassium ions and water molecules.* — K-1 and K-2 are the potassium ions belonging to double helices I and II, respectively, and each has three ligands (O-62B,

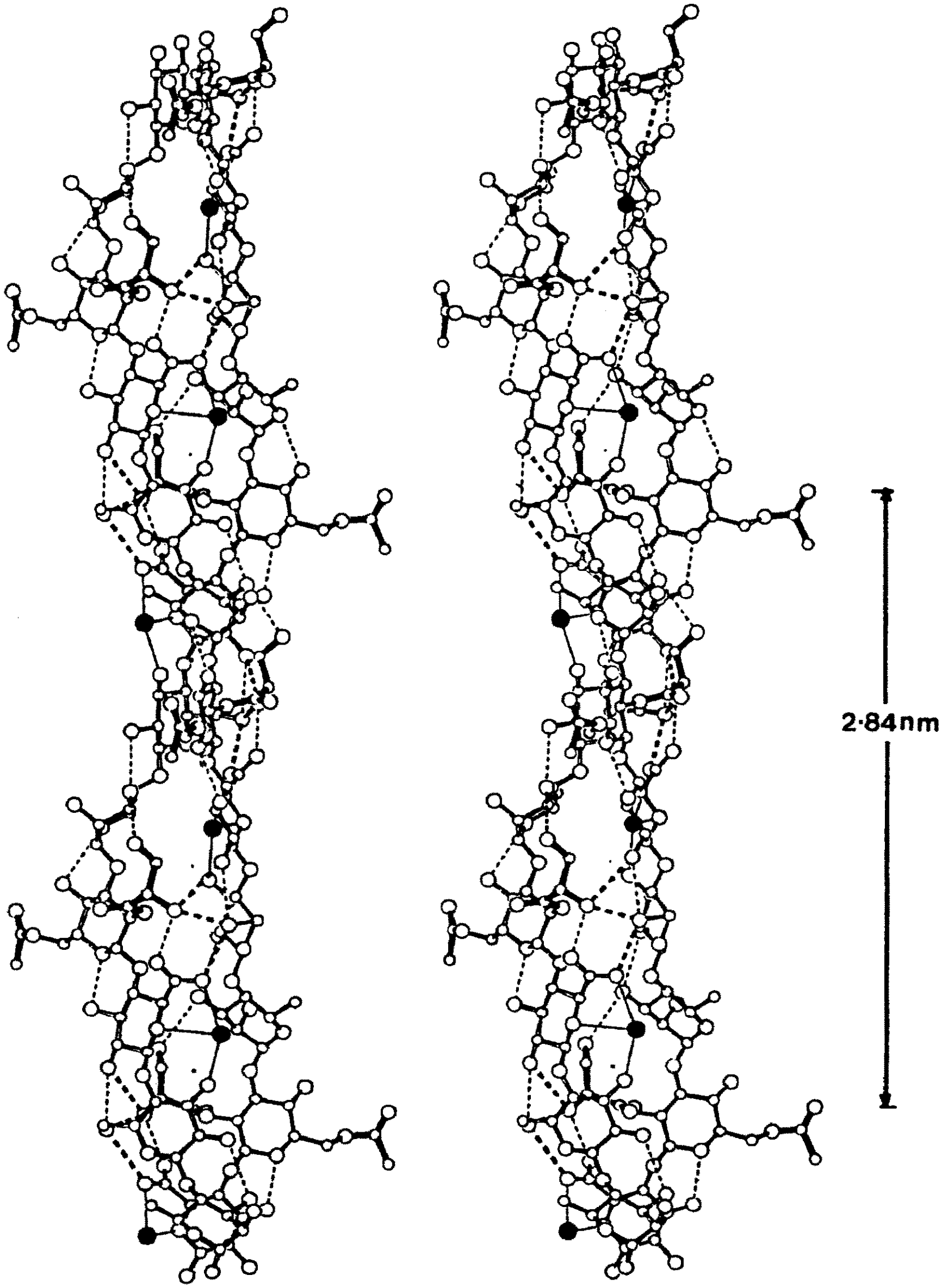
2·84nm

TABLE IV

Attractive interactions involving native gellan, potassium ions, and water molecules in the unit cell

| *Type* | *Atom X* | *Atom Y* | *X···Y (nm)* | *Atom P*[a] | *P-X···Y (°)* |
|---|---|---|---|---|---|
| Intrachain | O-3B | O-5A | 0.273 | C-3B | 101 |
| | O-2B | O-6C | 0.292 | C-2B | 135 |
| | O-4A | O-5D | 0.310 | C-4A | 94 |
| | O-3D | O-2C | 0.299 | C-3D | 103 |
| | O-10A | O-61B | 0.259 | C-10A | 102 |
| | O-11A | O-3D | 0.308 | C-11A | 103 |
| Interchain | O-6C | O-62B | 0.308 | C-6C | 106 |
| | O-6C | O-10A | 0.255 | C-6C | 135 |
| | O-2B | O-10A | 0.311 | C-2B | 133 |
| | O-2D(I) | O-2B(II) | 0.311 | C-2D | 147 |
| Ion and water | O-62B(I,1) | K-1 | 0.268 | C-6B | 103 |
| | O-5B(I,1) | K-1 | 0.283 | C-5B | 84 |
| | O-3C(I,1) | K-1 | 0.249 | C-3C | 133 |
| | O-62B(II,2) | K-2 | 0.254 | C-6B | 105 |
| | O-5B(II,2) | K-2 | 0.278 | C-5B | 90 |
| | O-3C(II,2) | K-2 | 0.270 | C-3C | 122 |
| | O-2B(II,2) | W-1 | 0.264 | C-2B | 127 |
| | O-6C(II,2) | W-1 | 0.291 | C-6C | 88 |
| | O-7A(II,1)(-1,-1) | W-1 | 0.250 | C-7A | 118 |
| | W-3 | W-1 | 0.300 | | |
| | O-11A(I,2) | W-2 | 0.270 | C-11A | 150 |
| | O-3D(I,2) | W-2 | 0.270 | C-3D | 146 |
| | W-2 | W-5 | 0.264 | | |
| | O-5D(I,2) | W-3 | 0.270 | C-5D | 101 |
| | O-4A(II,1)(0,-1) | W-3 | 0.245 | C-4A | 148 |
| | O-7A(II,1)(0,-1) | W-3 | 0.260 | C-7A | 112 |
| | O-2C(II,2)(0,-1) | W-4 | 0.277 | C-2C | 119 |
| | O-3C(II,2)(0,-1) | W-4 | 0.295 | C-3C | 100 |
| | O-5A(I,1) | W-5 | 0.284 | C-5A | 124 |
| | O-2C(I,2) | W-5 | 0.274 | C-2C | 114 |
| | O-3D(I,2) | W-5 | 0.278 | C-3D | 157 |

[a] P is the precursor of atom X. I and II, or 1 and 2, in parentheses after the atom name refer to the two double helices in the unit-cell, or the two chains in a double helix. The second set of parentheses includes unit-cell translations along *a* and *b*, respectively.

O-5B and O-3C) confined to only one chain. This arrangement is a major departure from the ion cage[16] which is necessary to establish the observed tight binding between gellan double helices. Table IV lists the interactions involving the ions and five water molecules with the surrounding double helices. The two water molecules W-1 and W-3

Fig. 3. A stereo view of the native gellan double helix. Light and dark bonds help to distinguish between the two chains. Thin and thick dashed lines denote intra- and inter-chain hydrogen bonds, respectively. Thin lines connect the potassium ion (filled circle) to its ligands. The glyceryl and acetyl groups are highlighted by thick bonds.

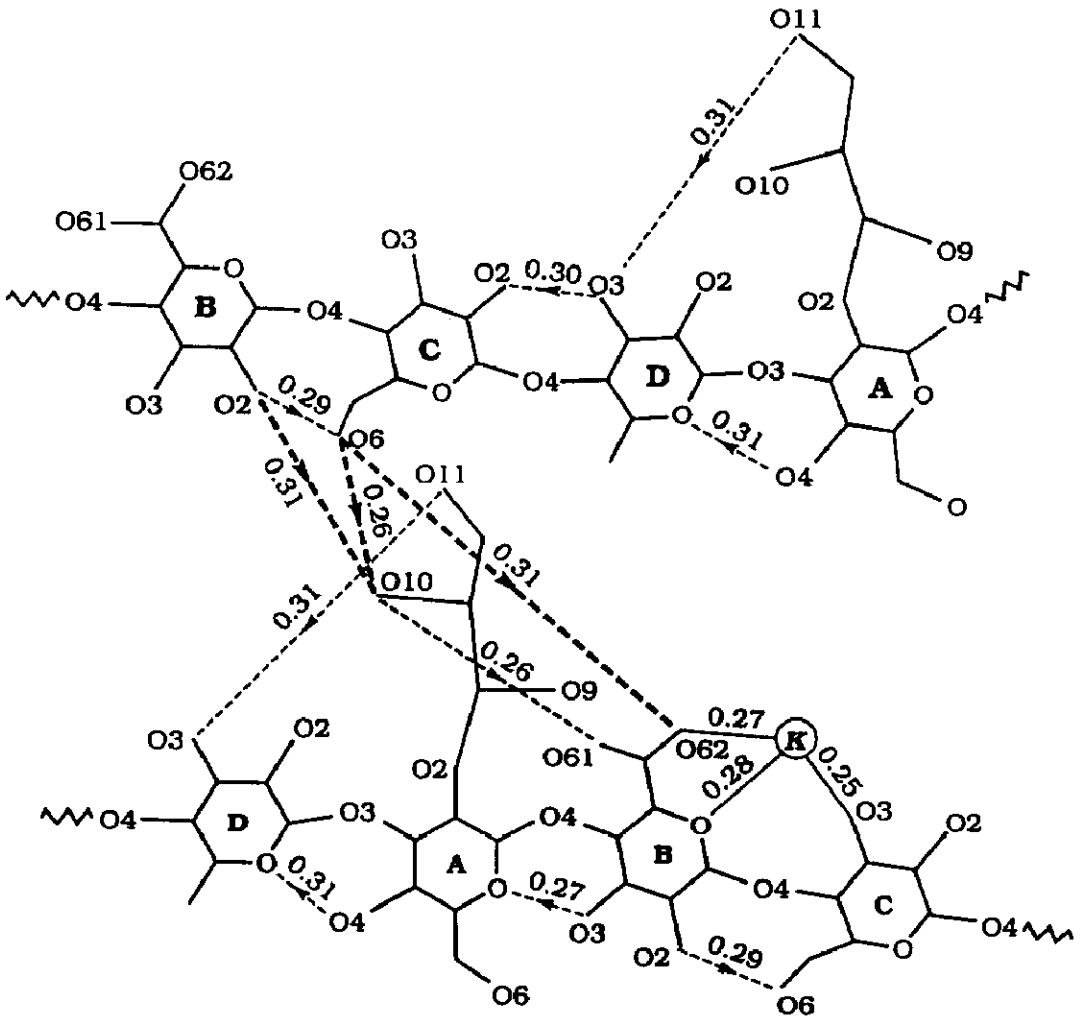


Fig. 4. Schematic illustration of the intra- (thin dashed line) and inter-chain (thick dashed line) hydrogen bonds and potassium ion (K) coordinated to its ligands (thin line) in the native gellan double helix. All distances are in nm.

participate in inter double helix interactions, which include the carbonyl oxygen atom in the terminal acetyl group. While W-2 and W-4 are confined to intrachain hydrogen bonds, W-5 is able to tie the two chains in the double helix. In addition, the water structure also exhibits self association *via* W-2···W-5 and W-1···W-3 bridges. All the hydrogen bonds within the double helix, and the ion-to-ligand distances, are schematically represented in Fig. 4. A close-up of the surroundings of the carboxylate group along with the potassium ion in native gellan is compared with that of gellan in Fig. 5. The most conspicuous feature is the large relative displacement of potassium from the ion cage in gellan, and this might be responsible for its weak gelation behavior.

*Molecular packing.* — The major intermolecular contacts are between glucuronate and rhamnose units. Since the intermolecular separation in the native unit cell (0.95 nm) is 0.05 nm more than in that of gellan, it is not surprising that there is only one inter double helix hydrogen bond O-2D(I)···O-2B(II), instead of three in the latter[8]. This implies that the aggregation of molecules will be weaker. There is no steric compression in the unit cell apart from one minor exception. The slightly short O-61B···O-9A contact (0.241 nm), between the two double helices, is presumably an artifact of the carboxylate shielding. Under protonated conditions, however, this might become a strong carboxyl-to-carbonyl oxygen hydrogen bond. Two mutually perpendicular views of the packing of molecules in the unit cell are depicted in Fig. 6 and Fig. 7a and they in general

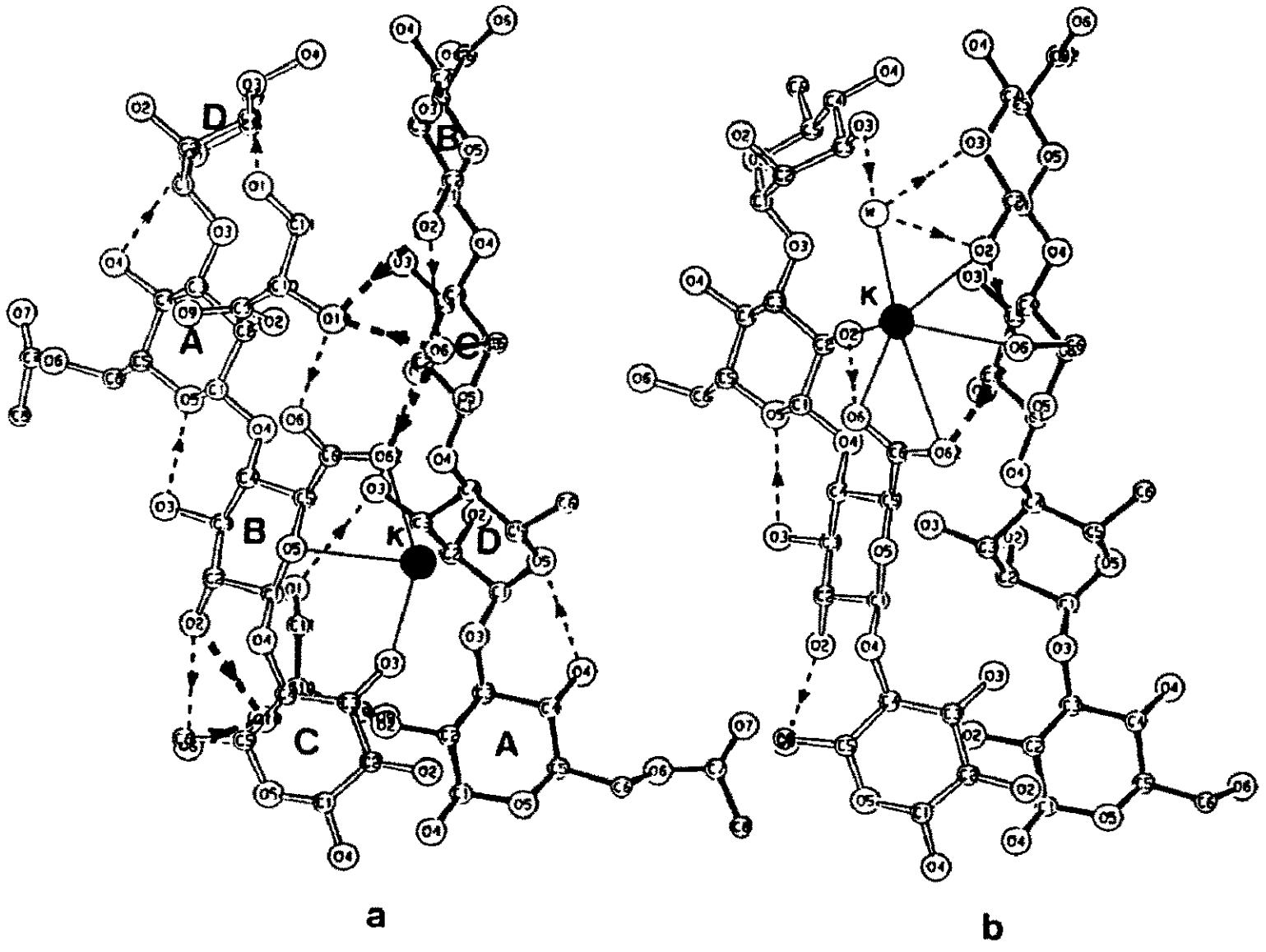


Fig. 5. A close-up view, normal to the helix axis, of a repeating unit per strand of (a) the native gellan double helix and its different ionic coordination, compared with that of (b) gellan[8]. Note that atoms O-10A and O-11A in (a) are almost at the same positions as K and W respectively, in (b).

resemble the corresponding views in potassium gellan[8]. The helix-axis projection (Fig. 6) brings out two important aspects. First, the peripheral acetyl groups stick into adjacent unit cells as predicted from modeling calculations[9]. Second, the cation sites are distinctly different from those in potassium gellan[8]. The side view (Fig. 7a) also reflects the same trend and is informative with regard to the associate properties of the native gellan double helices under monovalent, as well as divalent, ionic conditions.

## DISCUSSION

All gellan-related polysaccharides can form double-helical structures[16,17]. The details are gradually unfolding. This investigation reveals that the presence of acetyl or glyceryl groups does not interfere with double-helix formation, but does alter its ion-binding ability and also modify to some extent the gellan-like packing of the molecules in the unit cell. Within the slim double helix, the cellulose-like intrachain O-3B···O-5A, and the gellan-like interchain O-6C···O-62B, hydrogen bonds are preserved. Although there is an additional rotation of ~ 14° for the carboxylate group from the potassium gellan conformation, it is anchored in position by the intrachain O-10A···O-61B hydrogen bond.

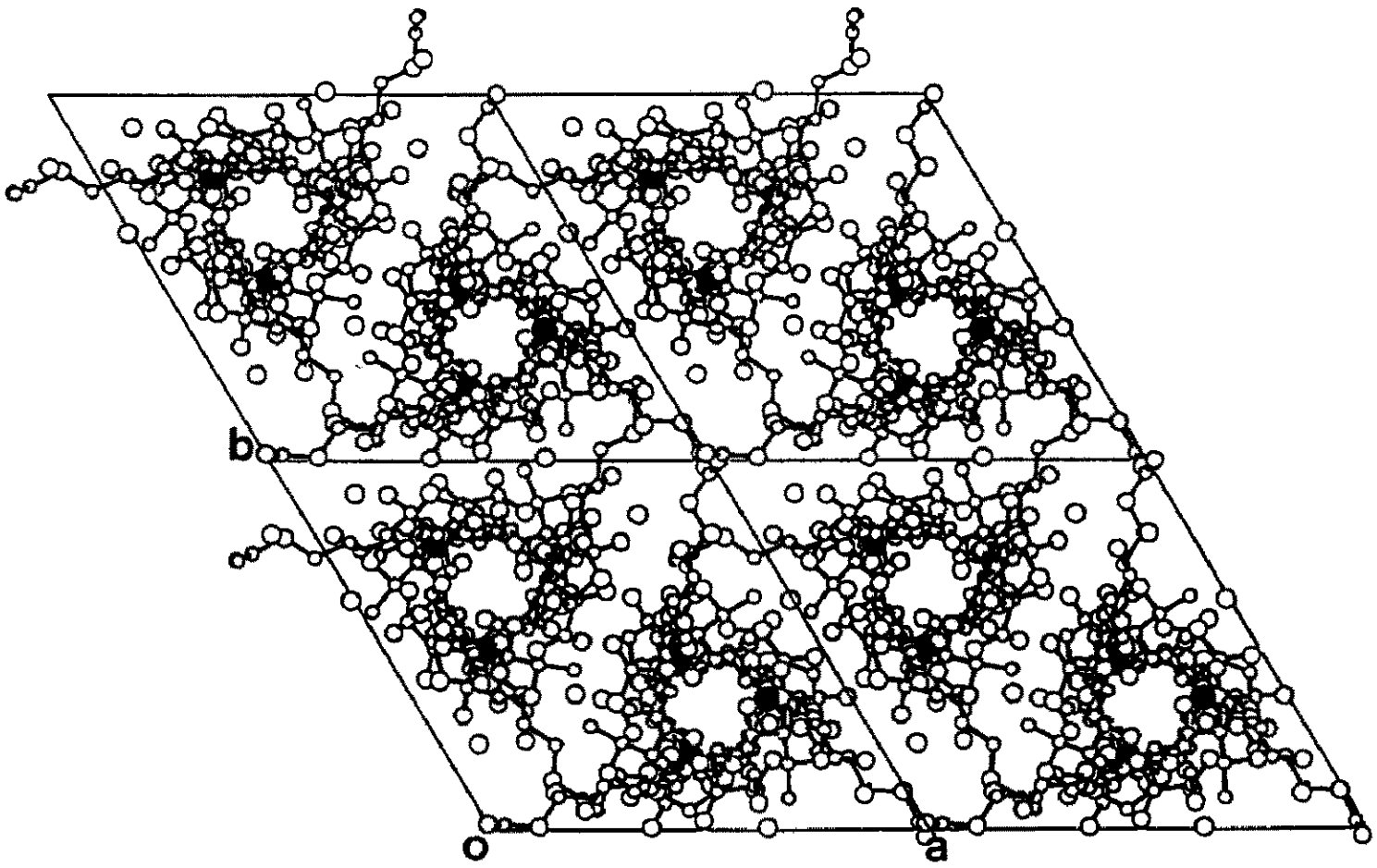


Fig. 6. A *c*-axis projection of four unit cells, each containing an up and a down native gellan double helix, the associated potassium ions (filled circles) and water molecules (open circles). The ions are ~0.1 nm closer to the helix axis than in potassium gellan[8]. The peripheral acetyl groups protrude into neighboring unit cells.

The interactions within the double helix, and between double helices, vividly suggest that the carboxylate group in every repeating unit is somwhat shielded from the solvent molecules and cations. In particular, the way the glyceryl group prevents the formation of the ion cage observed in potassium gellan[8,16] is intriguing. Atoms O-10A and O-11A (Fig. 5a) occupy the same positions as K and W (Fig. 5b), respectively in potassium gellan. Hence the three atoms O-61B, O-6C, and O-2B, out of a total of six ligands to the potassium ion, are able to form hydrogen bonds with atom O-10A. Only one atom O-3D, out of three hydrogen bonded to W, continues to do so with atom O-11A. This explains why the potassium gellan ion-cage does not prevail in native gellan. The net effect is considerable masking of the carboxylate group by the glyceryl moiety. Consequently, this will cause partial protonation on the carboxylate group, and the cation occupancy at a given site will be either zero or one. Since the primary structure itself has partial acetyl substitution (Fig. 1), it is not surprising that a statistical occupancy is also favored by the cation. The half occupancy for potassium, as deduced from the difference maps, is completely consistent with the environment of the carboxyl-(ate) and glyceryl groups. Therefore, we may expect the carboxylate and carboxyl groups to be present in nearly equal number in the fibers so that the p$K_a$ of native gellan will be higher than in gellan. This hypothesis is further supported by the relatively buried position of the carboxyl(ate) group and the consideration of coordination opportunities which are required for the gelation process. On this basis, we present below a plausible molecular origin for the weak gelation properties of native gellan.

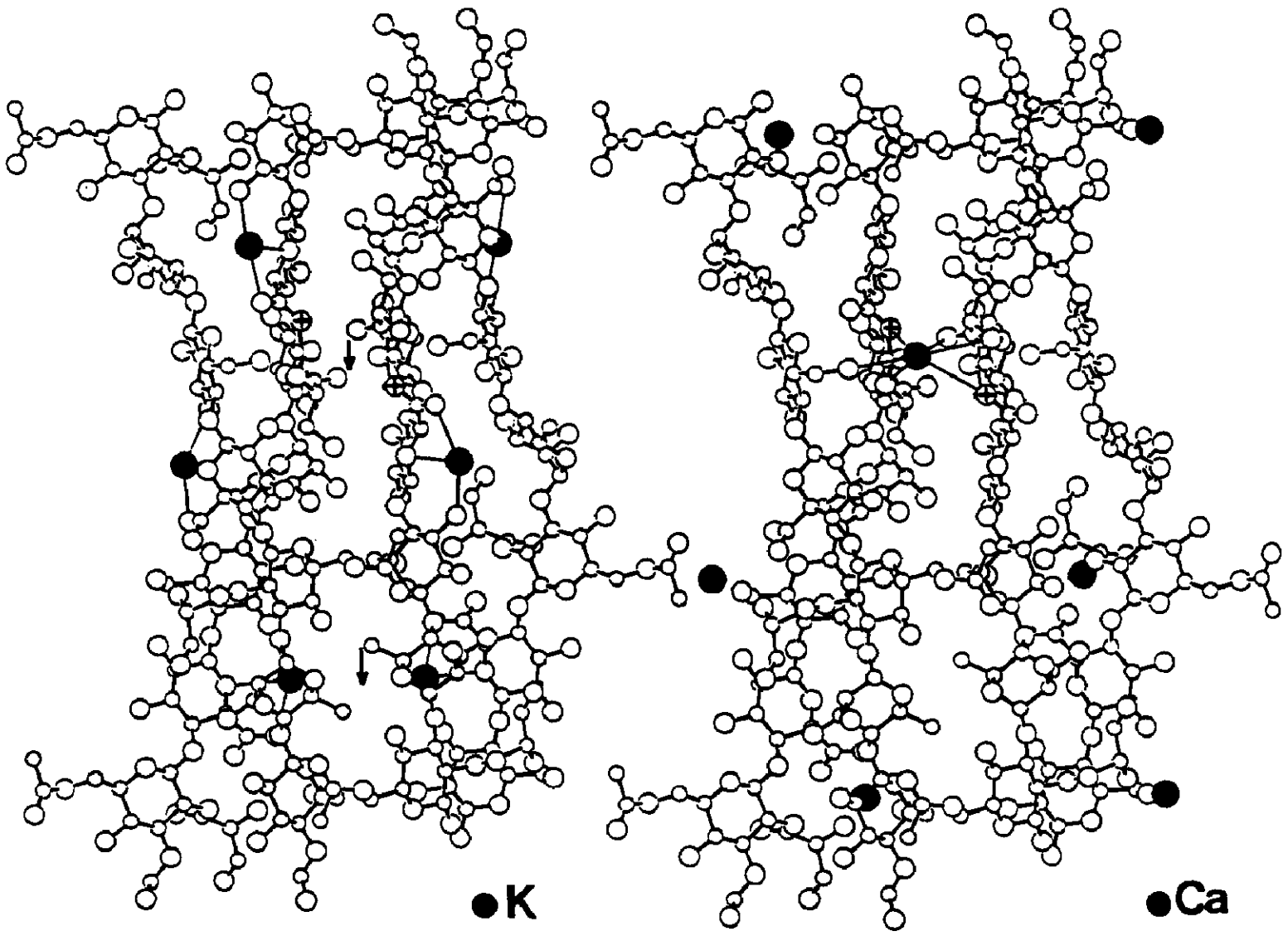


Fig. 7. (a) Packing of two potassium native gellan double helices in the unit cell viewed perpendicular to the helix axis. Potassium ions (filled circles) across the bottom arrow are 0.62 nm apart and the carboxylate oxygen atoms (crossed circles) across the top arrow are 0.53 nm apart. A putative calcium ion placed between these two oxygen atoms can possibly cross-link (thin lines) the double helices as in (b).

Fig. 7a indicates that pairs of potassium ions of half occupancy each appear in successive horizontal levels, roughly across the page, which are separated by 0.95 nm vertically. In the region near the closest approach of 0.53 nm (at the top arrow) of the carboxylate oxygens, one belonging to the up and the other to the down double helices, the carboxylate groups are oriented, face to face, as in potassium gellan[8]. But two potassium ions separated by about 0.43 nm, which are required for the gellan-like cross-linking of double helices *via* a water molecule, are not present between them. Near the bottom arrow, however, the opposite situation exists. The distance between the two potassium ions is 0.62 nm, 0.19 nm larger than in potassium gellan[8], and the associated carboxylate groups from the up and down double helices are pointed in opposite directions. In any case, there is no coordination between the carboxylate groups and the monovalent ions at either site, to meet the geometrical requirements for making the carboxylate···potassium···water···potassium···carboxylate interactions as efficiently as in potassium gellan[8] which would promote gelation. The lack of strong aggregation, therefore, reflects in native gellan's ability to form only weak and rubbery gels.

The two oxygen atoms which are 0.53 nm apart near the top arrow in Fig. 7a can be replaced by a single calcium and this leads to a putative model for calcium native gellan shown in Fig. 7b. The direct cross-linking of double helices involves three ligands from each to the ion. Among the six calcium-to-ligand distances, only one is 0.24 nm and the remaining five are between 0.30 and 0.34 nm. This cross-linking will be weaker than that in the calcium gellan model[9] in which three out of six are between 0.26 and 0.30 nm, and the other three between 0.30 and 0.33 nm. Once again, since the occupancy of the ion is only half, the cation-mediated gelation in native gellan will not be as strong as in gellan itself.

It has to be borne in mind that the above structural details emerging from our X-ray analysis correspond to one of the best choices for the ordered state of the polymer system. On the other hand, a crystal-structure model with an up and a down molecule, of half occupancy, at each site in the unit cell is another possibility, but the diagnostic streaks for such a statistical structure are however weak in the native gellan diffraction pattern. Therefore, this was not investigated. In solution, local domains may contain, for example, pairs of double helices packed in a parallel arrangement. Examination of such possibilities and their details must await further experimental evidence.

## CONCLUSIONS

X-Ray fiber diffraction analysis has shown that native gellan molecule exists as a half-staggered, parallel, double helix, similar to that of gellan. The glyceryl groups have a dominant role in stabilizing the double helix, in controlling the binding of cations to the double helix, and thus are responsible for the weak gelation behavior of the polymer. The acetyl groups, on the other hand, have no detectable structural role on its physical properties.

## ACKNOWLEDGMENTS

We thank Dr. Ralph Moorhouse and Mr. Ross Clark for helpful discussions, and Robert Werberig for photography. This work was supported in part by Kelco and the Industrial Consortium of the Whistler Center.

## REFERENCES

1 R. Moorhouse, in M. Yalpani (Ed.), *Industrial Polysaccharides: Genetic Engineering, Structure/Property Relations and Applications*, Elsevier, Amsterdam, 1987, pp. 187–206.
2 G. E. Sanderson, in G. O. Phillips, D. J. Wedlock, and P. A. Williams (Eds.), *Gums and Stabilizers for the Food Industry 5*, Oxford University Press, New York, 1990, pp. 333–344.
3 P. E. Jansson, B. Lindberg, and P. A. Sandford, *Carbohydr. Res.*, 124 (1983) 135–139.
4 H. Grasdalen and O. Smidsrød, *Carbohydr. Polymers*, 7 (1987) 371–393.
5 M.-S. Kuo, A. Dell, and A. J. Mort, *Carbohydr. Res.*, 156 (1986) 173–187.
6 V. Crescenzi, M. Dentini, and T. Coviello, *Carbohydr. Res.*, 149 (1986) 425–432.
7 R. Urbani and D. A. Brant, *Carbohydr. Polymers*, 11 (1989) 169–191.
8 R. Chandrasekaran, L. C. Puigjaner, K. L. Joyce, and S. Arnott, *Carbohydr. Res.*, 181 (1988) 23–40.
9 R. Chandrasekaran and V. G. Thailambal, *Carbohydr. Polymers*, 12 (1990) 431–442.

10 R. P. Millane and S. Arnott, *J. Appl. Crystallogr.*, 18 (1985) 419–423.
11 R. P. Millane and S. Arnott, *J. Macromol. Sci.-Phys.*, B24 (1985) 193–227.
12 P. J. C. Smith and S. Arnott, *Acta Crystallogr.*, A34 (1978), 3–11.
13 *International Tables for X-Ray Crystallography*, Kynoch Press, England, Vol. IV (1974) 99–101.
14 S. Arnott, R. Chandrasekaran, A. W. Day, L. C. Puigjaner, and L. M. Watts, *J. Mol. Biol.*, 149 (1981) 489–505.
15 W. C. Hamilton, *Acta Crystallogr.*, 18 (1965) 502–510.
16 R. Chandrasekaran, E. J. Lee, A. Radha, and V. G. Thailambal, in R. Chandrasekaran (Ed.), *Frontiers in Carbohydrate Research - 2*, Elsevier, London, 1991, in press.
17 E.J. Lee and R. Chandrasekaran, *Carbohydr. Res.*, 214 (1991) 11–24.